Entrainment temporal evolution across stably and unstably stratified vapor/clear air interfaces

ENTRAINMENT TEMPORAL EVOLUTION ACROSS STABLY AND UNSTABLY STRATIFIED VAPOR/CLEAR AIR INTERFACES.

Luca Gallana[1], Francesca De Santi[1], Silvio Di Savino[1], Renzo Richiardone[2], Michele Iovieno[1] & Daniela Tordella[1]

[1]*Dipartimento di Ingegneria Meccanica ed Aerospaziale, Politecnico di Torino, Torino, Italy*
[2]*Dipartimento di Fisica, Università di Torino, Torino, Italy*

Abstract Warm clouds as stratocumuli swathe a significant part of earth's surface and play a major role in the global dynamics of atmosphere by strongly reflecting incoming solar radiation so that an accurate representation of their dynamics is important in large-scale analyses of atmoshperic flows [9].The mixing and entrainment processes at the cloud top have been identified as fundamental to determine the internal structure of warm clouds, so that a clear and complete understanding of their physics is required [1]. The aim of this work is to study some of the basic phenomena which occur at a stratified interface focusing on the smallest scales of the flow which influence. These scales are important to understand the global dynamic of clouds, as pointed out by Malinowsky *et al.* [3]. To achieve the results, a campaign of high-resolution simulation of the local transport through a dry/moist air were performed by the means of Direct Numerical Simulations (DNS) using our home produced computational code that implements a de-aliased pseudospectral Fourier-Galerkin spatial discretization and an explicit low storage fourth order Runge-Kutta time integration scheme [2].

We consider the interface between clear air and moist air in a $6m \times 6m \times 12m$ parallelepipedic domain coupling two homogeneous and isotropic turbulent regions with different kinetic energy that interact through a mixing layer. The energy ratio is of the same order of the ones measured in warm clouds (see, e.g., [3]) and, furthermore, it allows us to compare our results with experiments on shearless mixing (see [8, 7]) in absence of any stratification. For each simulation two interfaces have been obtained, one in highly stably stratified condition, and one in unstable condition (see figure 1 for the flow configuration). The dynamics of interfaces is analyzed through an

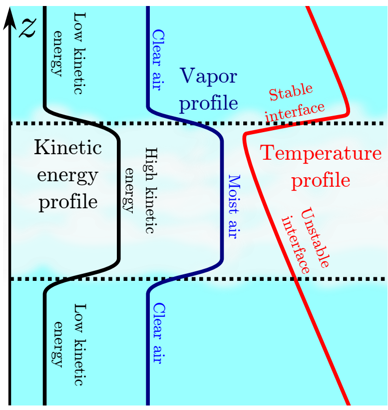

Figure 1. Scheme of the initial distribution along the vertical direction x_3 for the mean kinetic energy (black line), vapor concentration (blue line) and temperature profile (red line).

initial temperature perturbation located across one of the vapor/clear air interfaces thus generating a local stable layer, see red line in figure 1; the water vapor is treated as a passive scalar. The level of stratification is quantified with the Froude number, $Fr^2 = \frac{u_{rms}^2}{L^2 \alpha g \frac{dT}{dz}}$. For the stable cases, the Froude numbers considered ranges from 12.7 (weak stratification) to 0.6 (intense stratification), while for the unstable cases Fr^2 ranges from -250 to -16. In both stable and unstable cases the evolution of the system can be split in two different phases. In the first one, the buoyancy terms are negligible, and there are no significant differences with respect to a non-stratified case. As the system evolves, the effect of stratification becomes relevant (as soon as the stratification is intense).

About the unstable case layer we observe a high intermittency and an intense growth rate of the layer, which becomes overdiffusive in the case $Fr^2 = -16$. In particular, the entrainment, after an initial decay, asimptotically always shows a positive growth rate.

Here, for reason of space, we give details about the stably stratified layer which presents a more complex dynamics associated to the onset of a pocket very low turbulent kinetic energy. In figure 2, a visualization of the vertical velocity fluctuations in a portion of a vertical surface containing the stably stratified layer is shown. It can be observed the onset of a sub-layer characterized by the presence of low values of kinetic turbulent energy. At about 8 time scales, we observe the 8% of the energy in the wapor cloud and the 50% of the kinetic energy in the clear-air region. A similar trend was also observed in the LES cloud topped boundary layer simulations carried out by using Deardoff TKE model (NCAR group) and by using the ARAP TKE model (WVU group), [6]. The presence of such sublayer induces the formation of two local interfaces. Both of these interfaces present an intermittent behavior, and the entrainment (flux of dry air into the moist one) is blocked, as shown in figure 3, where the velocity of the moist air front w_e can be considered a characteristic parameter, since the entrainment of clear air is responsible of the growth of the cloud [4, 5]. As a consequence, the entrainment of clear air is confined to a thin interfacial layer. Also the dissipative terms inside the pit becomes relatively more important compared to the kinetic energy, making the pit deeper and deeper with respect to the external regions.

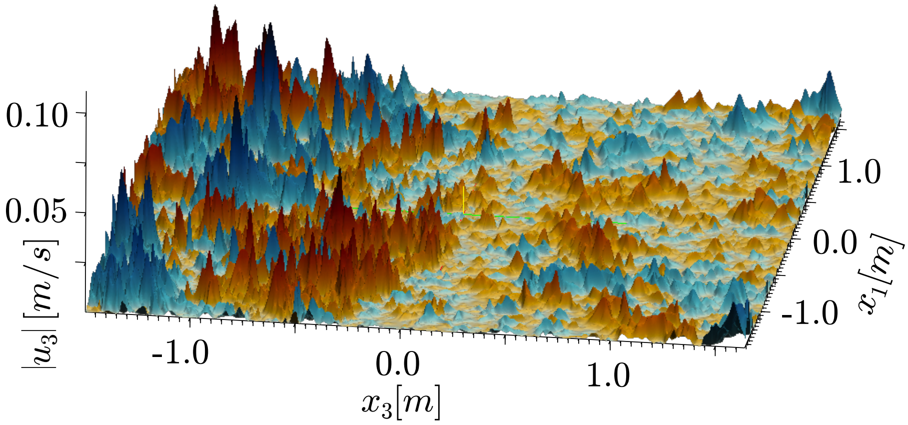

Figure 2. Elevation plot of the vertical component of the velocity in a vertical plane. The elevation is proportional to the square of vertical velocity fluctuations and the colors respect the velocity direction verse (blue for downward, red for upward). $Fr = 1.8$, 8 eddy turnover times. The formation of the pit of kinetic energy can be observed.

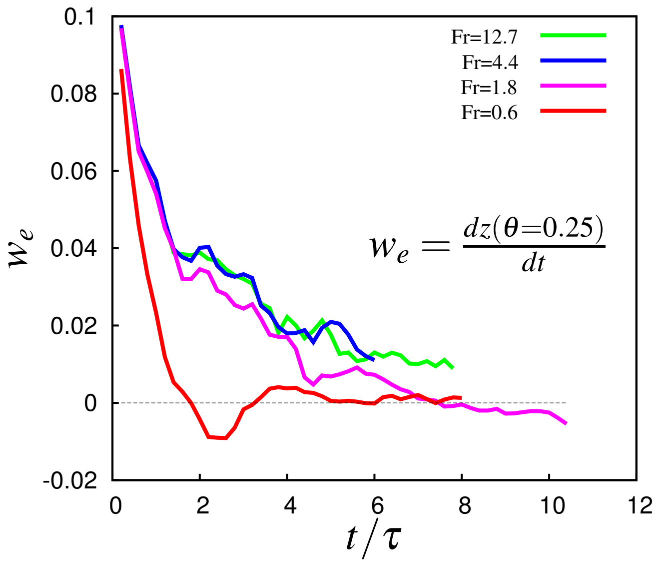

Figure 3. Evolution of the water vapor front vertical velocity w_e over time in case of stable stratification (different Fr are here represented). w_e is the time derivative of the horizontal plane where the mean water vapor concentation θ is equal to 0.25 and is a measure of the entrainment of dry air into the moist one.

References

[1] H. Gerber, G. Frick, Szymon P. Malinowski, H. Jonsson, D. Khelif, and Steven K. Krueger. Entrainment rates and microphysics in POST stratocumulus. *J. Geohys. Res. D*, **118**(21):12094–12109, NOV 16 2013.

[2] M. Iovieno, C. Cavazzoni, and D. Tordella. A new technique for a parallel dealiased pseudospectral Navier-Stokes code. *Comp. Phys. Comm.*, **141**:365–374, 2001.

[3] S. P. Malinowski, H. Gerber, I. Jen-La Plante, M. K. Kopec, W. Kumala, K. Nurowska, P. Y. Chuang, D. Khelif, and K. E. Haman. Physics of Stratocumulus Top (POST): turbulent mixing across capping inversion. *Atmos. Chem. Phys.*, **13**(24):12171–12186, 2013.

[4] Juan Pedro Mellado. The evaporatively driven cloud-top mixing layer. *J. Fluid Mech.*, **660**:5–36, OCT 10 2010.

[5] CH Moeng. Entrainment rate, cloud fraction, and liquid water path of PBL stratocumulus clouds. *J. Atmos. Sci.*, **57**(21):3627–3643, NOV 1 2000.

[6] CH Moeng, WR Cotton, C Bretherton, A Chlond, M Khairoutdinov, S Krueger, WS Lewellen, MK MacVean, JRM Pasquier, HA Rand, AP Siebesma, B Stevens, and RI Sykes. Simulation of a stratocumulus-topped planetary boundary layer: Intercomparison among different numerical codes. *Bull. Am. Meteorol. Soc.*, **77**(2):261–278, FEB 1996.

[7] D. Tordella and M. Iovieno. Small scale anisotropy in the turbulent shearless mixings. *Phys. Rev. Lett.*, **107**:194501, 2011.

[8] S. Veeravalli and Z. Warhaft. The shearless turbulence mixing layer. *J. Fluid Mech.*, **207**:191–229, 1989.

[9] Robert Wood. Stratocumulus Clouds. *Mon. Weather Rev.*, **140**(8):2373–2423, AUG 2012.